Journal of Food and Drug Analysis

Volume 32 | Issue 4 Article 9

Bitter acids from Humulus lupulus L. alleviate D-galactose induced osteoblastic senescence and bone loss via regulating AKT/mTOR-mediated autophagy

ORIGINAL ARTICLE

Bitter acids from *Humulus lupulus* L. alleviate D-galactose induced osteoblastic senescence and bone loss via regulating AKT/mTOR-mediated autophagy

Tian-Shuang Xia [a,1], Sheng-Yan Xu [a,1], Li-Yong Lai [a,1], Yi-Ping Jiang [a], Na-Ni Wang [b], Hai-Liang Xin [a,*]

[a] School of Pharmacy, Naval Medical University, Shanghai, 200433, China
[b] Department of Medicine, Zhejiang Academy of Traditional Chinese Medicine, Hangzhou, Zhejiang, 310007, China

Abstract

Bitter acids (BA) are main component of *Humulus lupulus* L. (hops). They are known for beer brewing and have various biological and pharmacological properties, especially the bone-protective effect confirmed by our previous *in vivo* study. Here we aimed to elucidate the anti-senior osteoporosis (SOP) effect of BA on osteoblasts and explore its underlying mechanism. *In vitro* SOP model was established by D-galactose (D-gal) injured osteoblasts, and the bone formation markers and apoptosis level were measured. mCherry-EGFP-LC3 adenovirus infection and autophagic markers including beclin1 and LC3 proteins were detected to investigate the autophagy level in osteoblasts. To further verify whether BA play the bone-protective role through regulating autophagy, the autophagy inhibitor 3-MA was used, and the cell proliferation, ALP activity, bone mineralization, apoptosis rate and SA-β-gal staining areas were measured. Finally, the protein expressions of AKT/mTOR signaling pathway were detected by Western blotting, and AKT agonist SC79 and mTOR agonist MHY1485 were used to further study the mechanism of BA on AKT/mTOR-mediated autophagy. The results showed that BA stimulated osteoblastic differentiation and inhibited apoptosis proteins Bcl-2/Bax in D-gal-treated osteoblasts. BA also increased the expression of autophagic markers beclin1 and LC3-II/LC3-I in D-gal-treated osteoblasts. mCherry-EGFP-LC3 autophagic double fluorescent adenovirus showed BA promoted the generation of autolysosomes and autophagosomes in D-gal-injured osteoblasts, indicating that BA might prevent osteoblastic bone loss through activating autophagy. Autophagy inhibitor 3-MA was used to further verify whether BA played the bone-protective role via regulating autophagy. The results revealed the promotion effects of BA on proliferation, ALP activity, and mineralized nodule formation in D-gal-injured osteoblasts were eliminated after autophagy blocking with 3-MA, and the inhibitory effects of BA on apoptosis rate and SA-β-gal staining areas were also eliminated. Moreover, BA reduced the phosphorylation levels of AKT, mTOR, p70S6K, and 4EBP in AKT/mTOR pathway, and the promotion of BA on the autophagic markers was blocked after the activation of AKT and mTOR by SC79 and MHY1485. In conclusion, it was the first time to demonstrate that BA improved cell activities and bone formation in aging osteoblasts, and revealed the mechanism of BA against SOP in osteoblasts was activating AKT/mTOR-mediated autophagy.

Keywords: AKT/mTOR pathway, Autophagy, Bitter acids, D-galactose, Senior osteoporosis

1. Introduction

Senior osteoporosis (SOP) is a kind of metabolic disease characterized by osteopenia, bone micro-structure degeneration and fracture. It can cause a series of complications and increase the mortality rate of the elderly, which is a crucial public health problem to be solved [1]. Bone is a dynamic organ with continuous remodeling occurring as bone formation and bone resorption. A decrease in bone formation and an increase in bone resorption result in bone loss. Current clinical drug treatments for bone loss and SOP mainly include estrogen therapy, bisphosphonates supplementation, as well

Received 12 December 2023; accepted 13 May 2024.
Available online 15 December 2024

* Corresponding author.
E-mail address: hailiangxin@163.com (H.-L. Xin).
[1] These authors contributed equally to this work.

https://doi.org/10.38212/2224-6614.3508

as calcium and active vitamin D, which cause more side effects and lack a clear target [2]. Therefore, it is urgent to elucidate the pathogenesis of SOP and find appropriate alternative drugs for SOP with few adverse effects.

Humulus lupulus L. (common name "hops"), an edible plant known for beer brewing, is also a traditional Chinese folk medicine for the treatment of female menopausal disorders, insomnia and forgetfulness [3]. In Europe, hops is widely used for hot flushes during menopause and postmenopausal osteoporosis [4]. More interestingly, it has been confirmed that moderate consumption of beer has positive effects on skeletal health, which is mainly attributed to bitter acids (BA) in hops. BA are the main components of hops, accounting for 5–20% [5]. As shown in Fig. 1, BA are mainly composed of α-acids (such as humulones) and β-acids (such as lupulones), both of which are prenylated phloroglucinol derivatives [6]. It has been demonstrated that BA possess various biological and pharmacological properties, including anti-inflammatory, anticancer, and anti-angiogenesis effects [7–9]. More interestingly, our previous study also confirmed that BA could protect against SOP via activating Nrf2/HO-1/NQO1 pathway and relieving oxidative stress in D-galactose (D-gal) induced aging mice [10]. However, the deep therapeutic mechanism still needs to be elucidated.

Aging is a main pathogenic factor causing SOP, which can trigger changes in many physiological processes in the body, such as oxidative stress, autophagy, and estrogen levels [11]. Among these physiological processes, autophagy is the primary cellular pathway for organelle, lipid, and long-lived protein degradation and recycling [12]. During autophagy, damaged proteins and organelles can be sequestered, degraded into their constituent parts within the lysosomes, and recycled as bioenergetic substrates. As a stress-responsive mechanism, the role of autophagy in maintaining homeostasis extends beyond an individual cell type or tissue to the whole organism [13]. Numerous studies have shown that autophagy is one of the key mechanisms regulating aging and increasing autophagy moderately can delay the occurrence of age-related diseases, such as SOP [14]. Therefore, the activation of autophagy has appropriately become a new strategy for preventing and treating SOP. Previous studies have confirmed the role of hops in activating autophagy to ameliorate memory impairment and prevent aging-related diseases [15]. Therefore, as the main component of hops, BA are speculated to have the potential to prevent SOP via regulating autophagy.

Additionally, osteoblast is a primary functional cell involved in bone remodeling, whose activity and bone formation ability are influenced by autophagy [16]. In the process of bone remodeling, the proliferation, differentiation and mineralization of osteoblast jointly affect bone formation, thereby maintaining bone homeostasis. Optimal

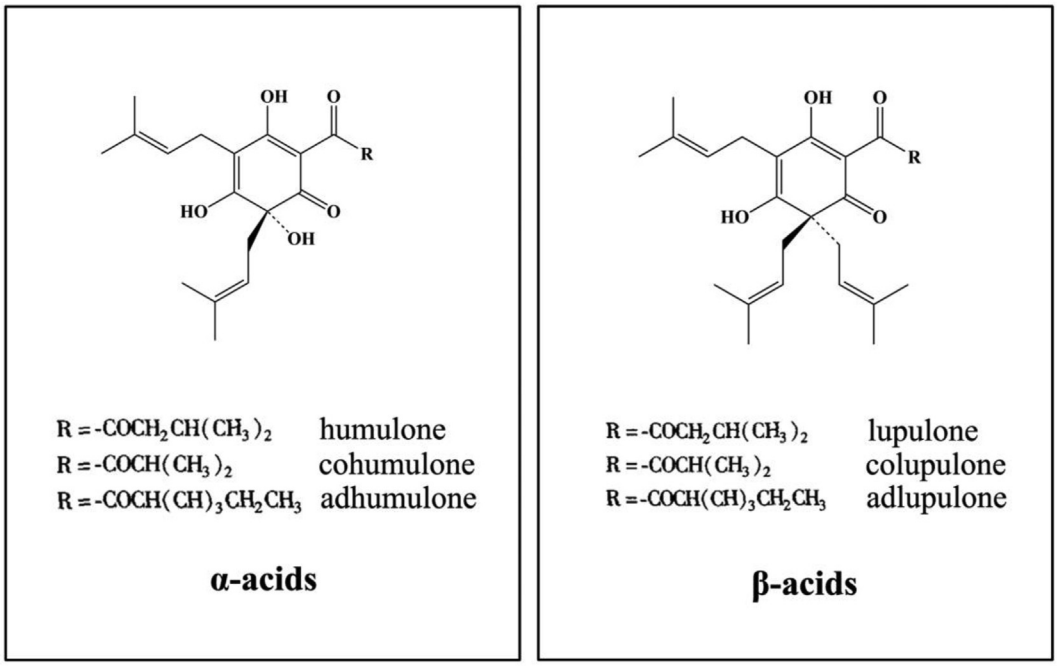

Fig. 1. Chemical structure of BA from hops.

differentiation of osteoblasts is associated with a later stage of AKT/mTOR signaling axis-mediated autophagy activation [17]. Conversely, inhibition of autophagy directly decreases the osteoblast differentiation and further induces bone loss [18]. Moreover, osteoblast is responsible for bone formation to produce osteoid and then mineralize with Ca^{2+} deposition accompanied with activated autophagy. The induction of autophagy during mineralization is required to meet the high-energy demands of active osteoblasts and removal of the misfolded bone-matrix proteins [19]. Our previous study have preliminarily clarified that BA can prevent bone loss by promoting osteoblastic differentiation and mineralization [20], but the mechanism is unclear. Accordingly, this study was to investigate the osteoprotective effect of BA on aging osteoblasts, and probe into its potential mechanism on regulating autophagy, which hopes to provide insights into the new molecular mechanism of BA against SOP.

2. Materials and methods

2.1. Reagents

BA standard extracts (cohumulone: 13.88%, n + adhumulone: 30.76%, colupulone: 13.44%, n + adlupulone: 10.84%) were purchased from American Society of Brewing Chemists (ICE-3, St. Paul, MN, USA). D-gal (MB1853) was purchased from Dalian Meilun Biotechnology Co., Ltd. (Dalian, Liaoning, China). 3-MA (5142-23-4) was purchased from Shanghai Yuanye Biotechnology Co., Ltd (Shanghai, China). SC79 (305834-79-1) and MHY1485 (326914-06-1) were purchased from Shanghai Aladdin Biochemical Technology Co., Ltd (Shanghai, China).

2.2. Cell culture and dosing regimen

Primary osteoblasts were acquired from skulls of newborn Wistar rats (Shanghai Sippr-BK laboratory animal Co. Ltd, Shanghai, China) and cultivated under the condition according to our previous experimental protocol [21]. The dosing regimen was as follows: D-gal (100 mmol/L), BA (2×10^{-9} mg/mL, 10^{-8} mg/mL, 5×10^{-8} mg/mL), 3-MA (10 mmol/L), SC79 (5 μg/mL) and MHY1485 (10 μmol/L). Cells were incubated with or without above drugs for 48 h. All animal studies were performed in line with the guidelines established by Institutional Animal Care and approved by the Committee on Ethics of Medical Research in Naval Military Medical University (No.202102624).

2.3. Western blot

Osteoblasts (1×10^5/mL) were seeded in 6-well plates and cultured overnight. Thereafter, cells were grouped and administrated for 48 h according to the dosing regimen mentioned above. Total cellular proteins were extracted with cell lysis buffer at centrifugation of 1000 r/min for 10 min. The quantified proteins were separated through sodium dodecyl sulfate-polyacrylamide gel electrophoresis and blotted onto polyvinylidene fluoride membranes. After blocked by 5% nonfat milk for 1 h at room temperature, membranes were incubated with primary antibodies overnight at 4 °C. Rabbit monoclonal antibodies of beclin1, LC3B, p-AKT, AKT, p-mTOR, mTOR, p-p70S6K, p70S6K, p-4EBP1, 4EBP1, GAPDH (Cell Signaling Technology, Danvers, MA, USA), RUNX2, BMP2, Bcl-2 and Bax (Beyotime Biotechnology Co., Ltd, Shanghai, China) were diluted at 1: 1000. In the next day, membranes were incubated with HRP-goat anti-rabbit IgG (1: 10000, BK-R050, Bioker Biotechnology Co., Ltd, Hangzhou, Zhejiang, China) for 1 h and imaged with enhanced chemiluminescent reagents. The band density was quantified by Image J software. GAPDH was used as an internal reference.

2.4. mCherry-EGFP-LC3 adenovirus infection

The mCherry-EGFP-LC3 adenovirus was used to monitor autophagy flux because the double fluorescence mCherry (red) and EGFP (green) in adenovirus can label LC3. Osteoblasts (2.5×10^4/mL) were cultured in 24-well plates for 24 h to reach around 50% confluence. Osteoblasts in each well were infected with 250 μL medium containing mCherry-EGFP-LC3 (MOI: 500, Hanbio company, Shanghai, China). After 4 h of culture, cells were added with another 250 μL culture medium and continuously infected for 8 h. Cells were then treated with reagents for 48 h and observed by confocal microscope. EGFP is quenched with the pH change caused by the fusion of autophagosome and lysosome. Six cells in each group were selected to count the yellow and red dots. The experiment was repeated three times.

2.5. MTT assay and alkaline phosphatase (ALP) assay

Osteoblasts were seeded in 96-well plates at the density of 1×10^4/mL and incubated overnight. Cells were then treated with reagents for 48 h. Proliferation of osteoblasts was measured by MTT (Boguang Biotechnology Co., Shanghai, China) at the end of

treatment (Zhang et al., 2019). ALP activity in osteoblast supernatant was determined by ALP assay kit (Jiancheng Bioengineering Institute, Nanjing, China). For ALP staining, osteoblasts (2×10^4/mL) were seeded in 6-well plates. After the same administration as MTT experiment, intracellular ALP was stained according to the instruction of BCIP/NBT ALP color development kit (Beyotime Biotechnology Co., Ltd, Shanghai, China). The stained cells were observed and photographed under microscope.

2.6. Alizarin red staining

Osteoblasts were seeded in 24-well plates at the density of 1×10^4/mL. To stimulate the formation of bone mineralized nodules, cells were firstly cultured in medium containing β-glycerophosphate (10 mmol/L), L-ascorbic acid (50 μg/mL) and dexamethasone (1 μmol/L) for 18 days. After additional administration for 6 days, specimens were stained with Alizarin red S (Yuanye Biotechnology Co., Ltd, Shanghai, China) and photographed under microscope. Bone nodules in each well were dissolved by 500 μL 10% cetylpyridine chloride, then 100 μL from each hole were taken for measurement. The optical density reflecting the bone mineralization ability was determined at 570 nm.

2.7. Apoptosis rate detection and β-galactosidase staining

Osteoblasts (1×10^5/mL) were seeded in 6-well plates overnight and followed by treatment with reagents for 48 h. For apoptosis rate, osteoblasts were detached and centrifuged at 200 g for 5 min at room temperature. After the cells suspended with PBS and re-collected under the same centrifugation condition, corresponding fluorescent dyes were added according to the apoptosis kit (Beyotime Biotechnology Co., Ltd, Shanghai, China). The apoptosis rate was detected by flow cytometry. On the hand of β-galactosidase staining, osteoblasts were fixed and added with dyeing working solution according to the instruction of β-galactosidase staining kit (Beyotime Biotechnology Co., Ltd, Shanghai, China). After incubated overnight at 37 °C without CO_2, cells were photographed under microscope. The blue stained areas reflecting senescence were quantified with Image J software.

2.8. Molecular docking

The mTOR crystal structure (PDB ID: 4DRI) composed of peptidylproline isomerase FKBP5, FRB protein and rapamycin was obtained from RCSB protein data bank (https://www.rcsb.org/) and Uniprot database (https://www.uniprot.org/). Before molecular docking, molecules of Rapamycin and water in this structure were discarded while hydrogen atoms were added as the final receptor with PyMol software. The 3D structures of humulone, cohumulone, adhumulone, lupulone, colupulone and adlupulone were downloaded from the PudChem database (https://www.ncbi.nlm.nih.gov/pccompound/) as ligands. Analog docking of receptor and ligands were performed by Autodock 4.2. The chemical interactions were analyzed and presented with Ligplot and PyMol software.

2.9. Statistical analyses

Data were expressed as means ± standard error of the mean (SEM) of at least three independent experiments and multiple comparisons of measurement data were performed with one-way analysis of variance (ANOVA). GraphPad Prism 5.0 software was used for data analysis, and statistical significance was set at $p < 0.05$.

3. Results

3.1. BA promoted osteoblastic differentiation and inhibited apoptosis in D-gal-treated osteoblasts

RUNX2 and BMP2 take important parts in regulating osteoblast differentiation and maturation. Bcl-2 and Bax are crucial apoptosis-regulating proteins, which are antagonistic to each other to maintain the balance between apoptosis and anti-apoptosis. As shown in Fig. 2, compared with the control group, the expressions of RUNX2, BMP2 and Bcl-2/Bax decreased significantly in D-gal-treated osteoblasts. The administration of BA (2×10^{-9} mg/mL, 10^{-8} mg/mL, 5×10^{-8} mg/mL) significantly improved the expression of RUNX2, and BA (10^{-8} mg/mL, 5×10^{-8} mg/mL) improved the expression of BMP2 and Bcl-2/Bax in D-gal-treated osteoblasts. BA at the concentration of 2×10^{-9} mg/mL slightly increased the expression of BMP2 and Bcl-2/Bax in D-gal-injured osteoblasts, but there was no statistical difference. These results indicated the role of BA in promoting osteoblastic differentiation and inhibiting apoptosis.

3.2. BA promoted autophagy in D-gal-treated osteoblasts

Expressions of autophagic markers including beclin1 and LC3 proteins were detected to investigate the level of autophagy in osteoblasts. As shown

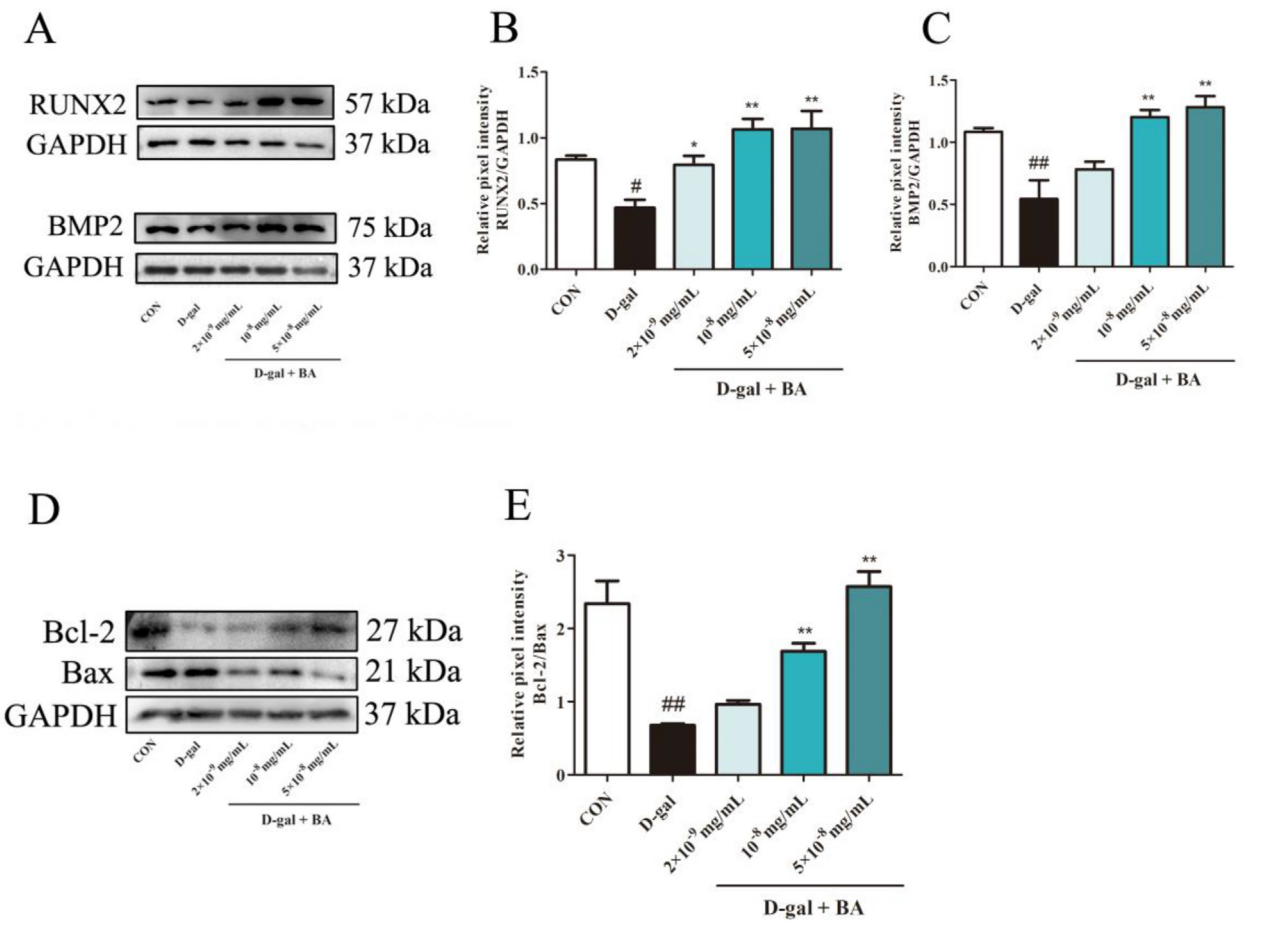

Fig. 2. Effects of BA on the expressions of RUNX2, BMP2, Bcl-2 and Bax in D-gal-treated osteoblasts. (A–C) Western blot and quantitative analysis of RUNX2 and BMP2, (D–E) Western blot and quantitative analysis of Bcl-2 and Bax (n = 3). $^{\#}p < 0.05$ vs. CON, $^{\#\#}p < 0.01$ vs. CON, $^{*}p < 0.05$ vs. D-gal, $^{**}p < 0.01$ vs. D-gal by ANOVA test.

in Fig. 3 A-C, D-gal significantly reduced the expressions of beclin1 and LC3-II/LC3-1 in osteoblasts, while BA (10^{-8} mg/mL, 5×10^{-8} mg/mL) significantly increased the expression of beclin1 in D-gal-injured osteoblasts. BA at 2×10^{-9} mg/mL slightly increased the expression of beclin1, but there was no statistical difference. All doses of BA significantly up-regulated the ratio of LC3-II/LC3-I in D-gal-treated osteoblasts. Additionally, autophagic flux was detected by mCherry-EGFP-LC3 autophagic double fluorescent adenovirus. In Fig. 3D, the red spots indicate the formation of autolysosomes and the yellow ones merged from red-green spots represent autophagosomes. Compared with the control group, the number of yellow spots (Zoom) and red spots (mCherry) decreased significantly in D-gal-treated osteoblasts, indicating the decline of autophagic flux. With the presence of BA (10^{-8} mg/mL, 5×10^{-8} mg/mL), the number of yellow and red spots were both significantly increased (Fig. 3D and E), indicating that BA increased the expression of autophagosome and autolysosome, and stimulated the flow of autophagosome towards autolysosome, further promoting autophagy of osteoblasts.

3.3. BA protected osteoblasts against D-gal-induced injury through activating autophagy

Autophagy inhibitor 3-MA was used to further verify whether BA played the protective role through activating autophagy. As shown in Fig. 4, after autophagy blocking with 3-MA, the promotion effects of BA on proliferation, ALP activity, expression of RUNX2 and BMP2, and mineralized nodule formation in D-gal-injured osteoblasts were eliminated. Meanwhile, as shown in Fig. 5, after autophagy blocking with 3-MA, the inhibitory effects of BA on apoptosis rate and SA-β-gal staining areas in D-gal-treated osteoblasts were also eliminated. These results further proved that in D-gal-injured osteoblasts, BA protected the cell function by promoting autophagy so as to prevent the osteoblastic senescence and apoptosis.

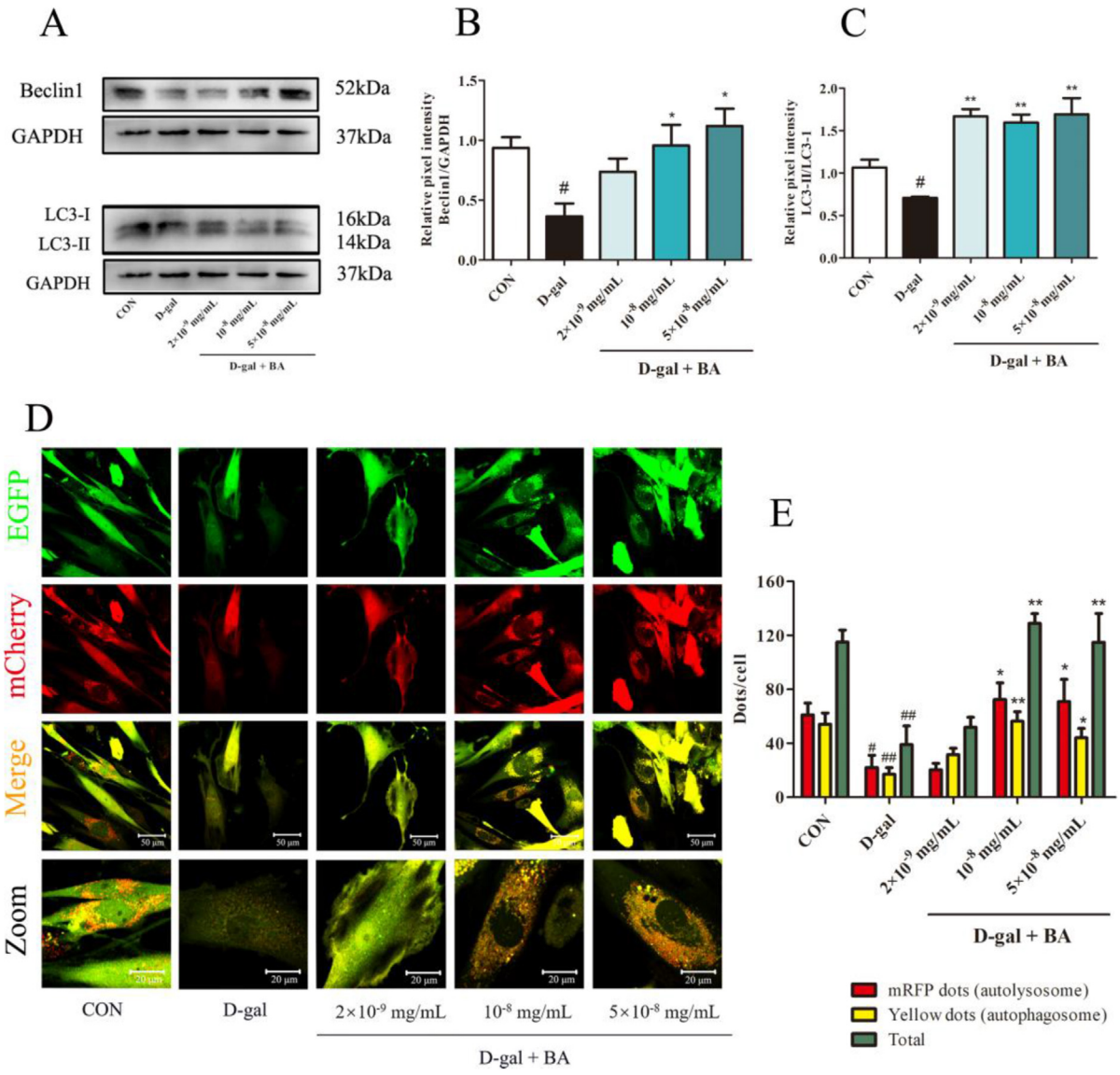

Fig. 3. Effects of BA on autophagy in D-gal-treated osteoblasts. (A–C) Western blot and quantitative analysis of Beclin1 and LC3-II/LC3-I, (D) representative images of osteoblasts infected with mCherry EGFP-LC3 double fluorescent adenovirus (scale bar: 50 μm 63 ×, 20 μm 176.4 ×), (E) quantitative analysis on LC3 dots (n = 3). $^{\#}p < 0.05$ vs. CON, $^{*}p < 0.05$ vs. D-gal, $^{**}p < 0.01$ vs. D-gal by ANOVA test.

3.4. Molecular docking analysis of mTOR to chemical structures of BA

The minimum binding energy, hydrogen bonding and hydrophobic interactions of the best binding site between FKBP5/FRB domain and each ligand were shown in Table 1. The minimum binding energy of adhumulone and FKBP5/FRB domain was lower than −5 kcal/mol, and the ones of humulone, cohumulone, lupulone, colupulone, adlupulone and FKBP5/FRB domain were lower than −7 kcal/mol. As shown in Fig. 6, hydrogen bonds were formed between Rapamycin and six amino acid residues of FKBP5, including Arg73, Gly84, Gln85, Ile87, Tyr113. Five of them also formed hydrogen bonds with BA, which were Arg73: humulone, Gln85: humulone and hopulone, Ile87: humulone, Tyr113: humulone. The functional groups of BA involved in the formation of hydrogen bonds are mainly acyl groups and hydroxyl groups in the ring structure. Rapamycin forms hydrophobic interaction with 17 amino acid residues of FKBP5/FRB domain, of which 14 can also form hydrophobic interaction with structures of BA, including Tyr57, Phe67, Phe77, Trp90, Ile122, Phe130, Leu2031, Glu2032, Ser2035, Phe2039, Trp2101, Asp2102, Tyr2105 and Phe2108. These results indicated the possibility of stable combination between mTOR and BA structures.

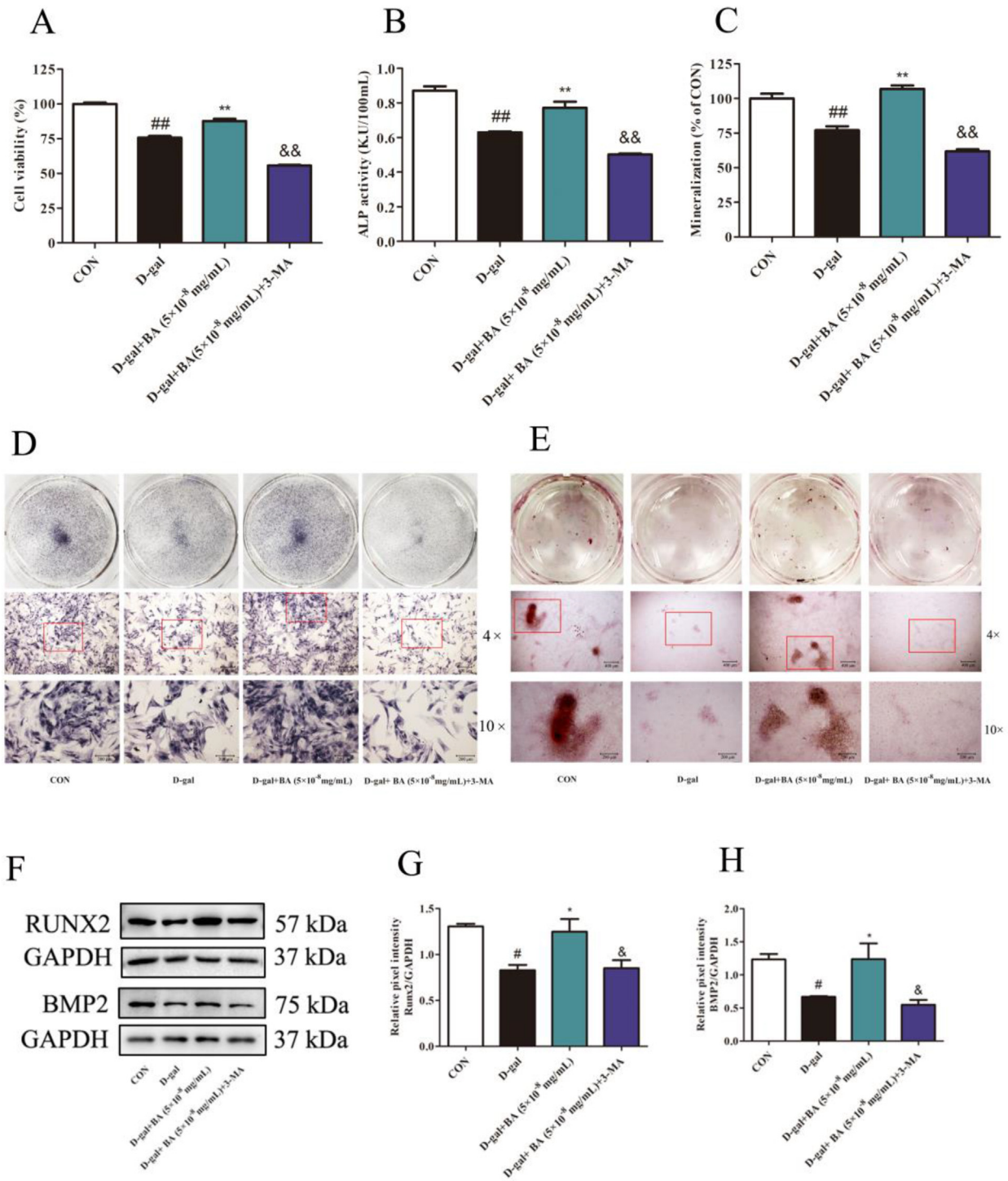

Fig. 4. Autophagy inhibitor 3-MA was used to verify whether BA exerted bone-protective effects through promoting autophagy. (A) Proliferation capacity of osteoblasts (n = 6), (B) ALP activity of osteoblasts (n = 6), (C) mineralization ability of osteoblasts (n = 3), (D) ALP staining of osteoblasts (scale bar: 400 μm 4 × , 200 μm 10 ×), (E) Alizarin red staining of mineralized nodules of osteoblasts (scale bar: 400 μm 4 × , 200 μm 10 ×), (F–H) Western blot and quantitative analysis of RUNX2 and BMP2 (n = 3). $^{\#}p < 0.05$ vs. CON, $^{\#\#}p < 0.01$ vs. CON, $^{*}p < 0.05$ vs. D-gal, $^{**}p < 0.01$ vs. D-gal, $^{\&}p < 0.05$ vs. D-gal + BA (5×10^{-8} mg/mL), $^{\&\&}p < 0.01$ vs. D-gal + BA (5×10^{-8} mg/mL) by ANOVA test.

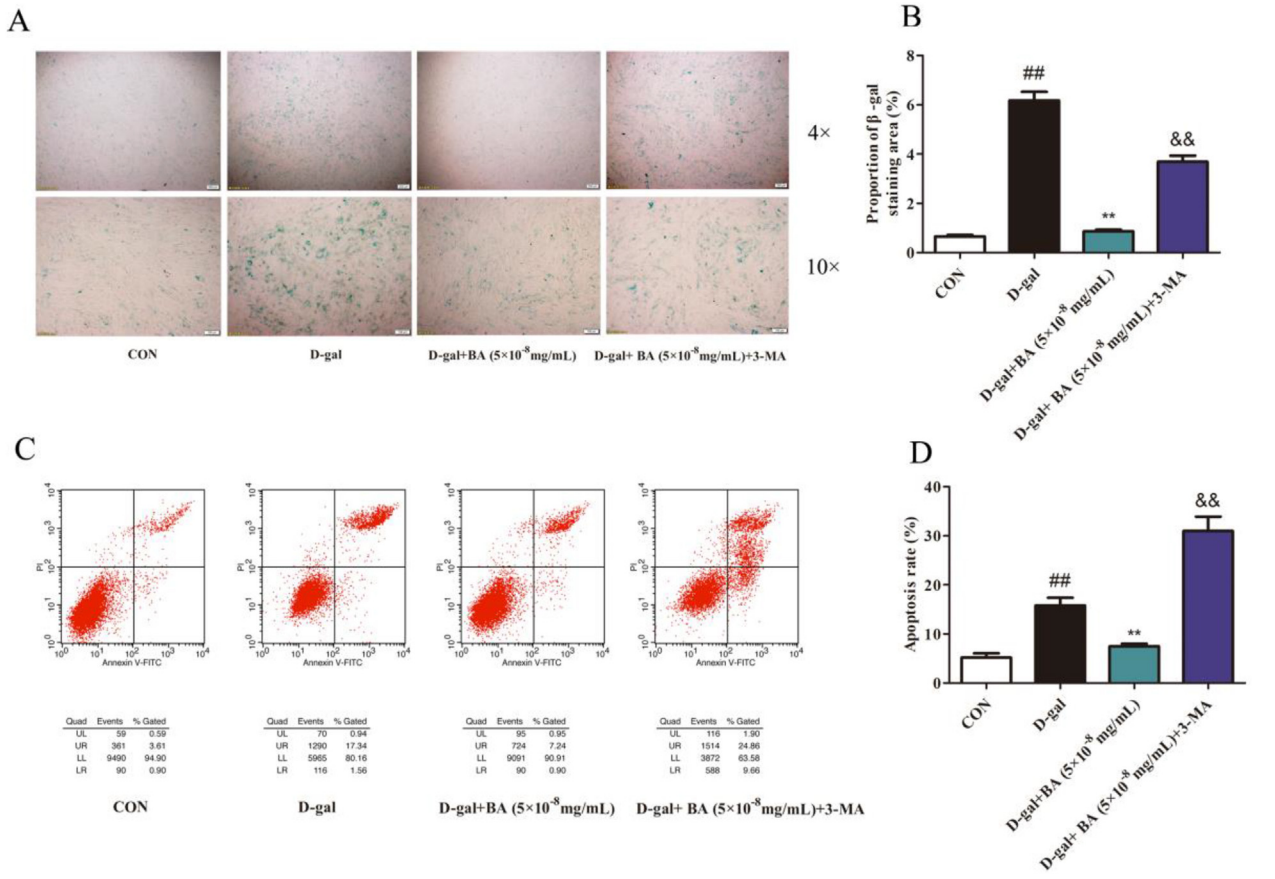

Fig. 5. Effects of BA on the apoptosis and senescence of D-gal-treated osteoblasts. (A) Photography of senescence-associated β-galactosidase staining (scale bar: 400 μm 4 × , 200 μm 10 ×), (B) proportion of β-galactosidase staining (n = 3), (C–D) apoptosis rate detected by flow cytometry. $^{\#\#}p < 0.01$ vs. CON, $^{**}p < 0.01$ vs. D-gal, $^{\&\&}p < 0.01$ vs. D-gal + BA (5×10^{-8} mg/mL) by ANOVA test.

Table 1. Intermolecular interaction between BA and FKBP5/FRB domain.

Ligands	Docking Score (kcal/mol)	Hydrogen Bonds	Hydrophobic Interactions
Rapamycin	−19.4	FKBP5: Asp68, Arg73, Gly84, Gln85, Ile87, Tyr113	FKBP5: Tyr57, Phe67, Phe77, Val86, Trp90, Ile122, Phe130 FRB: Leu2031, Glu2032, Ser2035, Phe2039, Gly2040, Thr2098, Trp2101, Asp2102, Tyr2105, Phe2108
Humulone	−7.45	FKBP5: Tyr57, Arg73, Tyr113, Ser118	FKBP5: Phe67, Asp68, Phe77, Trp90, Leu119, Lys121, Ile122, Phe130 FRB: Asp2102
Cohumulone	−7.34	FKBP5: Gln85 FRB: Ser2035	FKBP5: Lys52, Val78, Phe79 FRB: Leu2031, Glu2032, Arg2036, Trp2101, Tyr2105, Phe2108, Arg2109, Ser2112
Adhumulone	−6.78	FKBP5: Ile87	FKBP5: Phe77, Phe79, Gln85, Val86, Trp90, Tyr113, Ser118, Phe130 FRB: Phe2039, Tyr2105
Lupulone	−7.7	FKBP5: Gln85 FRB: Ser2035	FKBP5: Val78, Phe79 FRB: Leu2031, Glu2032, Phe2039, Trp2101, Tyr2104, Tyr2105, Phe2108, Arg2109
Colupulone	−7.14	FKBP5: Ser118	FKBP5: Tyr57, Phe67, Arg73, Phe77, Gln85, Val86, Ile87, Trp90, Tyr113, Ile122, Phe130 FRB: Phe2039, Asp2102
Adlupulone	−8.12	FKBP5: Val78 FRB: 2035	FKBP5: Lys52, Arg73, Phe77, Phe79, Ser80, Gln85 FRB: Leu2031, Glu2032, Phe2039, Tyr2105, Phe2108, Arg2109, Ser2112

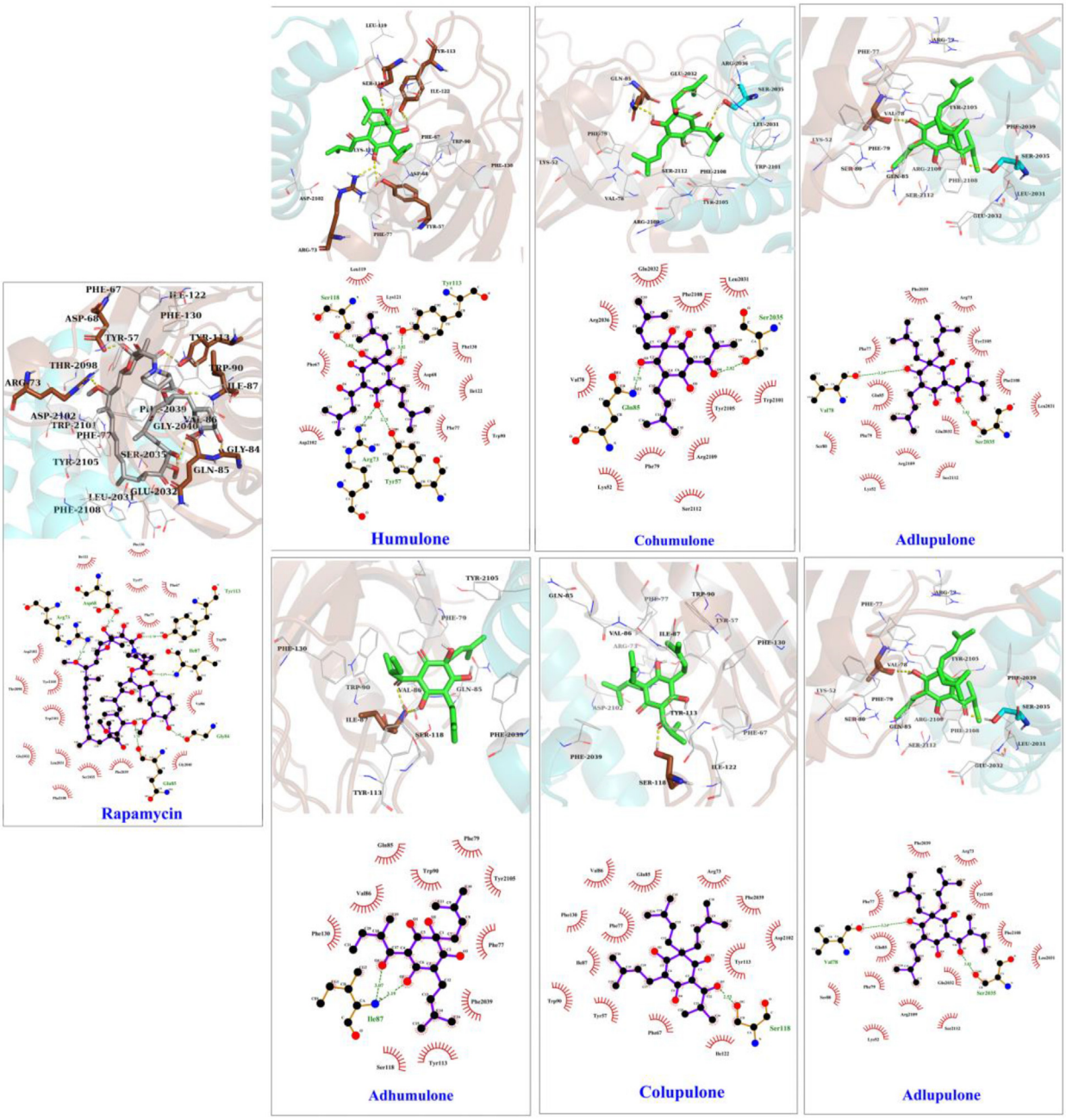

Fig. 6. Best binding sites of Rapamycin and BA structures to FKBP5/FRB domain.

3.5. BA regulated AKT/mTOR signaling pathway in D-gal-treated osteoblasts

The protein expressions in AKT/mTOR signaling pathway were detected by Western blotting to further study the mechanism of BA on autophagy. As shown in Fig. 7, after D-gal treatment, the phosphorylation levels of AKT, mTOR, p70S6K and 4EBP1 of osteoblasts were significantly increased. Administration of BA significantly reduced the phosphorylation levels of AKT, mTOR, p70S6K and 4EBP1 in D-gal-treated osteoblasts.

AKT agonist SC79 and mTOR agonist MHY1485 were used to further verify whether BA played a role through AKT/mTOR signal pathway. As shown in Fig. 8, the phosphorylation of mTOR, p70S6K and 4EBP1 inhibited by BA were reactivated by AKT and mTOR agonists. Accordingly, the promotion of BA on the autophagic markers beclin1, LC3-II/LC3-1 in D-gal injured osteoblasts was blocked after the activation of AKT and mTOR. These results indicated BA promoted autophagy by inhibiting AKT/mTOR signaling pathway.

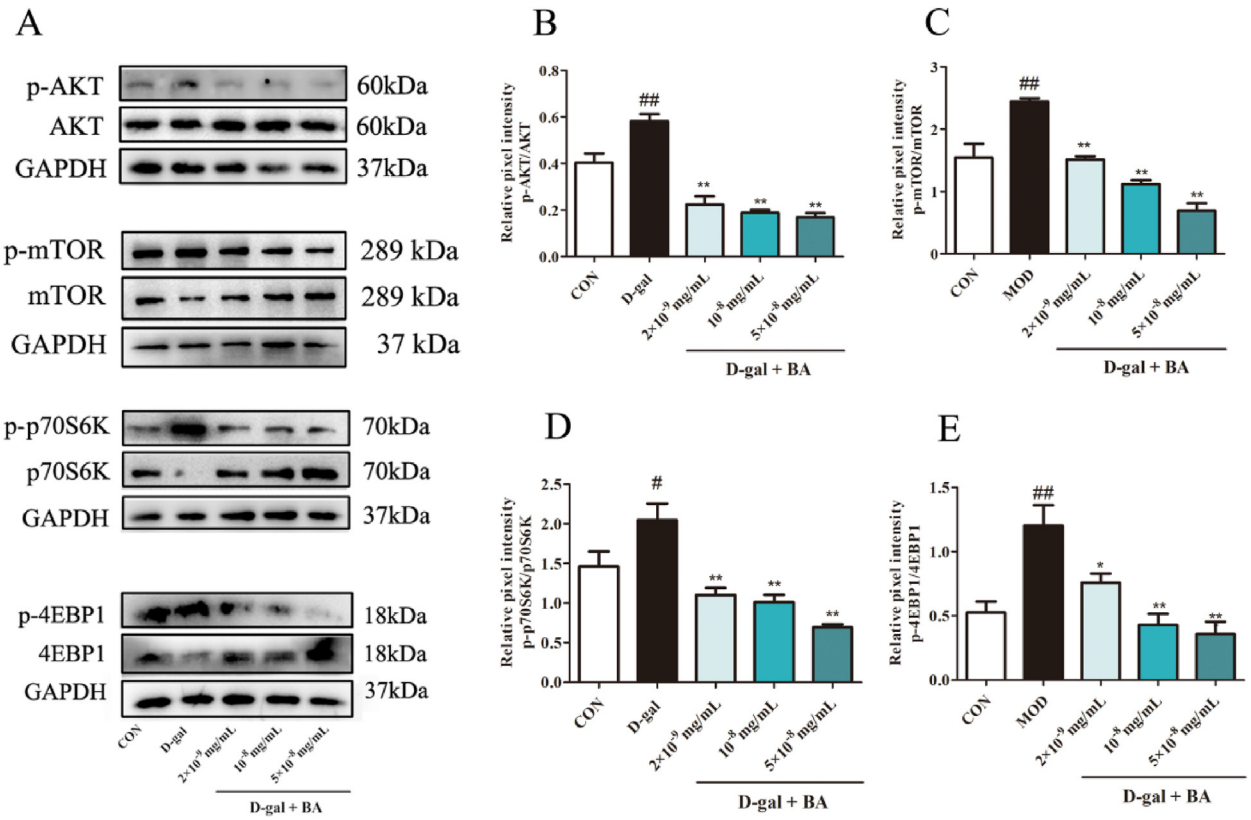

Fig. 7. Effects of BA on AKT/mTOR signaling pathway in D-gal-treated osteoblasts. (A–E) Western blot and quantitative analysis of p-AKT/AKT, p-mTOR/mTOR, p-p70S6K/p70S6K and p-4EBP1/4 EBP1 (n = 3). $^{\#}p < 0.05$ vs. CON, $^{\#\#}p < 0.01$ vs. CON, $^{*}p < 0.05$ vs. D-gal, $^{**}p < 0.01$ vs. D-gal by ANOVA test.

4. Discussion

The elderly have high risk for osteoporosis. Autophagy abnormality induced by osteoblastic senescence is crucial in the occurrence and development of SOP. BA are the main components of hops with multiple pharmacological functions including anti-inflammation, anti-oxidation, anti-tumor, and anti-angiogenesis. Our previous study also confirmed that BA could relieve oxidative stress and protect against SOP in aging mice. In this study, we firstly discovered that BA improved cell activities and bone formation in aging osteoblasts, and revealed the mechanism of BA against SOP in osteoblasts was activating AKT/mTOR-mediated autophagy.

D-gal is a kind of natural reducing sugar in human body and many foods. Since the characteristics of least side effects, convenience, and higher survival rate throughout the experimental period, D-gal is the optimal choice to induce aging model such as SOP, and it has been reported that D-gal can induce osseous changes and bone loss during aging [22]. During the process of SOP, decreased bone formation of osteoblasts plays a key role [23]. Osteoblasts participate in the synthesis, secretion, and mineralization of bone matrix. *In vitro* culture system of osteoblasts undergoes three stages: cell proliferation, extracellular matrix differentiation and maturation (type I collagen, non-collagen proteins, enzymes, growth factors, etc.), and matrix mineralization [24]. The final differentiated osteoblasts are embedded in the bone matrix and are the main source of bone cells. Therefore, detection of osteoblastic proliferation, differentiation and mineralization abilities can reflect the function on bone formation. In this study, D-gal injured osteoblasts were used to establish an *in vitro* SOP model, and it was discovered that BA could promote the proliferation, differentiation, and mineralization of D-gal injured osteoblasts, indicating that BA can improve bone formation in aging osteoblasts.

Senescence and apoptosis are also vital factors affecting the function of osteoblasts. Studies have found that the number and activity of osteoblasts decrease as aging, further leading to the decline of age-related bone mass [25]. Osteoblasts senescence is an important factor inducing SOP. Osteoblasts apoptosis is a programmed cell death that plays a crucial role in bone development and maintenance,

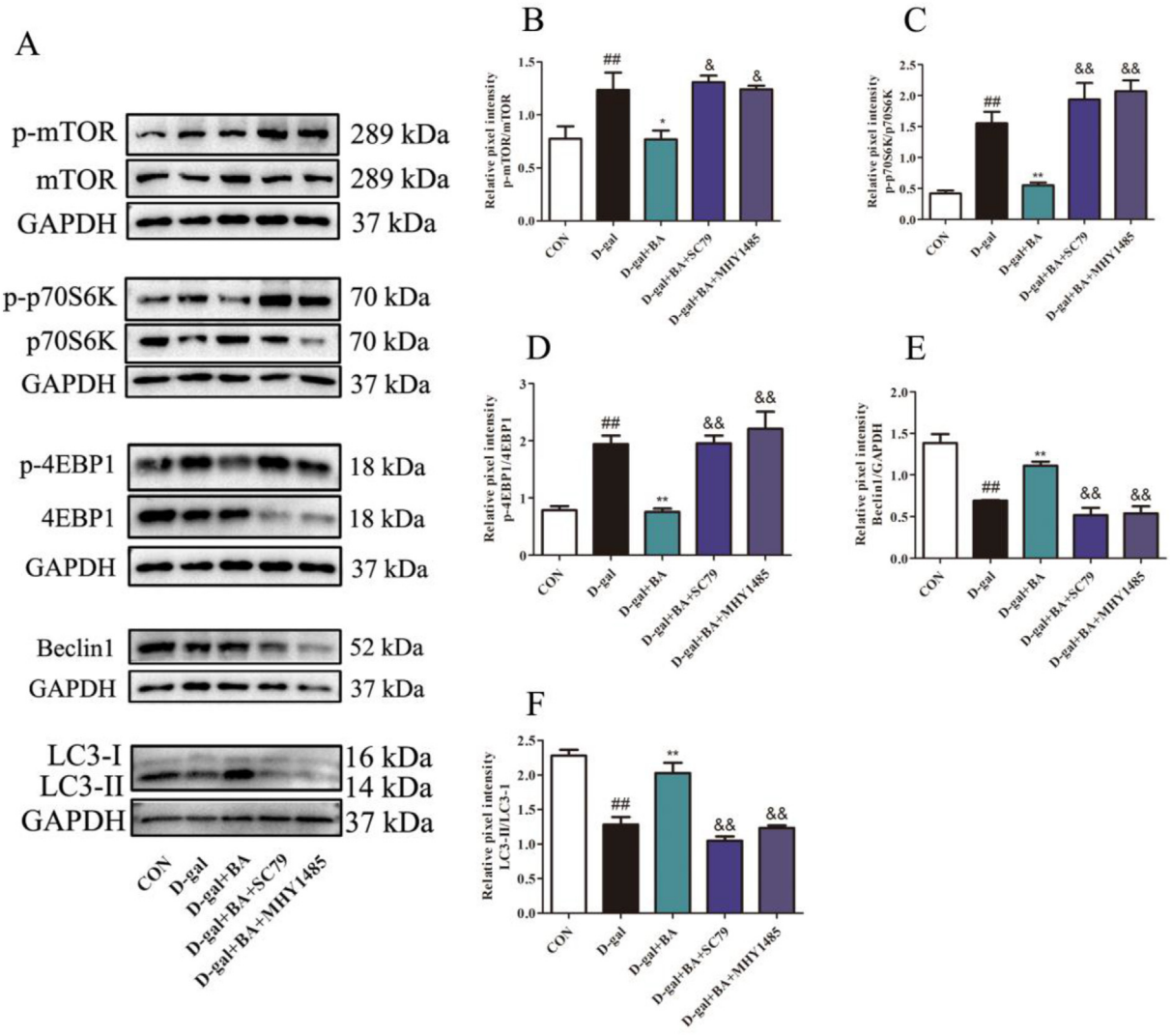

Fig. 8. AKT agonist SC79 and mTOR agonist MHY1485 were used to verify whether BA exerted effects through promoting AKT/mTOR-mediated autophagy. (A–F) Western blot and quantitative analysis of p-mTOR/mTOR, p-p70S6K/p70S6K, p-4EBP1/4EBP1, beclin1 and LC3-II/LC3-I (n = 3). $^{\#\#}p < 0.01$ vs. CON, $^{*}p < 0.05$ vs. D-gal, $^{**}p < 0.01$ vs. D-gal, $^{\&}p < 0.05$ vs. D-gal + BA (5×10^{-8} mg/mL), $^{\&\&}p < 0.01$ vs. D-gal + BA (5×10^{-8} mg/mL) by ANOVA test.

and there is a closely correlation between bone loss caused by aging and apoptosis of osteoblasts [26]. Bcl-2 and Bax are both crucial apoptotic regulatory proteins that antagonize each other and maintain a balance between apoptosis and anti-apoptosis by regulating the permeability of mitochondrial membranes. They can work together to change mitochondrial membrane potential and induce a series of pro apoptotic signals [27]. This study discovered that D-gal promoted the senescence and apoptosis of osteoblasts, while BA effectively alleviated this senescence and apoptosis state, thereby protecting the function of damaged osteoblasts, suggesting BA can protect osteoblasts from senescence and apoptosis, thereby preventing and treating SOP.

Autophagy is a highly conserved self-degradative and energy dynamic recycling process in the proliferation, differentiation and maturation of eukaryotic cells, which can provide energy and basic substances for cellular homeostasis and survival through degradation of cytoplasmic misfolded or aggregated proteins, damaged organelles or macro-molecules [28]. Studies have found that a decrease in autophagy levels can be observed in elderly tissues, and the decrease in autophagy levels can also lead to mice aging and the occurrence of SOP [14]. Our previous study also found that promoting autophagy in osteoblasts can effectively inhibit cell oxidative stress and apoptosis, thereby protecting osteoblast activities [29]. These can be seen that autophagy plays an

important role in retarding aging and preventing SOP. Specifically, the dynamic process of autophagy, also known as autophagic flux, is mainly regulated by autophagy-related genes (ATG), among which beclin1 (ATG6) and LC3 play core roles. In the process of autophagic flow, the dual fluorescence mCherry (red) and EGFP (green) in mCherry-EGFP-LC3 adenovirus can be used to label LC3, a key autophagy marker. After the fusion of autophagosomes and autolysosome, EGFP undergoes fluorescence quenching due to changes in pH, and only red fluorescence can be detected [30]. Therefore, the increase of red fluorescence indicates that autophagosome are flowing towards autolysosome, and autophagy is activated. In this study, BA could significantly increase the number of yellow (merged of red and green) and red spots in D-gal osteoblasts, indicating that BA stimulated the flow of autophagosome towards autolysosome, further promoting autophagy of osteoblasts.

Specifically, LC3 includes two forms, LC3-I and LC3-II. Among them, LC3-I can combine with PE to form LC3-II under the action of ATG12-ATG5-ATG16L complex. Next, LC3-II is embedded in the membrane structure and participates in the extension and closure of autophagosome membrane [31]. Therefore, LC3-II/LC3-I is considered as a main marker reflecting the start of autophagy. However, the expression of LC3-II/LC3-I just suggests the normalcy of autophagosome formation, but cannot confirm the binding effect between autophagosomes and lysosomes [32]. Beclin1 is responsible for recruiting related ATG proteins to form autophagic vesicles with membrane structure, and promotes the localization of autophagy proteins to autophagosomes [33]. Therefore, the concurrent detection of LC3-II/LC3-I and beclin1 serves as a reliable indicator for the occurrence of autophagy. In this study, it was discovered that BA of middle or high doses significantly up-regulated LC3-II/LC3-I and beclin1 in D-gal-treated osteoblasts, indicating BA activated osteoblastic autophagy. However, low dose BA only had effects on increasing LC3-II/LC3-I, while no effects on promoting beclin1, suggesting it just activated the start of autophagy, instead of the entire process of autophagy. These results were similar to previous reports [34] and the mCherry-EGFP-LC3 autophagic double fluorescent adenovirus in this study. In addition, after treatment with autophagy inhibitor 3-MA, the positive effects of BA on osteoblasts activities were eliminated, indicating that BA protected osteoblasts function and promoted bone formation through activating autophagy level.

Additionally, autophagy is regulated by multiple molecules and signaling pathways, among which AKT/mTOR signaling pathway is a classic one that regulates cellular autophagy [35]. AKT is the upstream target of mTOR, and activation of AKT phosphorylation can stimulate mTOR, thereby inhibiting autophagy and increasing cell apoptosis [36]. As a redox-sensitive factor, mTOR is the intersection of multiple signaling pathways, which can simultaneously participate in the regulation of osteoblasts senescence and autophagy [37]. The stimulation of mTOR can directly induce the activation of two downstream target proteins, p70S6K and 4EBP1, and further inhibit autophagy [38]. During the process of osteoporosis, mTOR is found to participate in osteoblast differentiation and formation. Osteoblast proliferation was accompanied by increased mTOR phosphorylation, and mTOR signaling could be suppressed during osteoblasts differentiation. Apart from regulating osteoblasts differentiation, mTOR also acts as an excellent regulator in the proliferation, apoptosis, autophagy, energy metabolism, pleiotropic functions, and the maintenance of osteoblasts or osteoblast-like cells [39]. Additionally, Rapamycin, an mTOR inhibitor, was also found to increase BMD, suggesting that mTOR plays a negative role in bone grafting mediated by osteoblasts via inhibiting the differentiation or the bone formation at late stages [40]. This study discovered that BA significantly inhibited the phosphorylation of AKT, mTOR, p70S6K, and 4EBP1 in D-gal injured osteoblasts, and the suppressed mTOR, p70S6K, and 4EBP1 proteins was reactivated by AKT and mTOR agonists. Correspondingly, the promoting effect of BA on autophagy markers beclin1 and LC3-II/LC3-I was blocked after activation of AKT and mTOR, suggesting BA can alleviate D-gal induced osteoblastic senescence and SOP via AKT/mTOR-mediated autophagy.

5. Conclusion

It was demonstrated for the first time that BA could alleviate D-gal induced osteoblastic senescence and bone loss, and the molecular mechanism was related to activating AKT/mTOR-mediated autophagy. In combination with our previous research [10], we believe that BA are worth to be developed in the treatment of SOP.

Conflict of interest

The authors declare that they have no known competing financial interests or personal relationships that could have appeared to influence the work reported in this paper.

Acknowledgments

This work was supported by the National Natural Science Foundation of China (82174079, U1603283).

References

[1] Colón-Emeric CS, Hecker EJ, McConnell E, Herndon L, Little M, Xue T, et al. Improving shared decision-making for osteoporosis pharmacologic therapy in nursing homes: a qualitative analysis. Arch Osteoporos 2022;17:11.
[2] Vasto S, Baldassano D, Sabatino L, Caldarella R, Di Rosa L, Baldassano S. The role of consumption of molybdenum biofortified crops in bone homeostasis and healthy aging. Nutrients 2023;15:1022.
[3] Aghamiri V, Mirghafourvand M, Mohammad-Alizadeh-Charandabi S, Nazemiyeh H. The effect of Hop (*Humulus lupulus* L.) on early menopausal symptoms and hot flashes: a randomized placebo-controlled trial. Compl Ther Clin Pract 2016;23:130−5.
[4] Sasaoka N, Sakamoto M, Kanemori S, Kan M, Tsukano C, Takemoto Y, et al. Long-term oral administration of hop flower extracts mitigates Alzheimer phenotypes in mice. PLoS One 2014;9:e87185.
[5] Kao TH, Wu GY. Simultaneous determination of prenylflavonoid and hop bitter acid in beer lee by HPLC-DAD-MS. Food Chem 2013;141:1218−26.
[6] Hsu YY, Kao TH. Evaluation of prenylflavonoids and hop bitter acids in surplus yeast. J Food Sci Technol 2019;56: 1939−53.
[7] Chen WJ, Lin JK. Mechanisms of cancer chemoprevention by hop bitter acids (beer aroma) through induction of apoptosis mediated by Fas and caspase cascades. J Agric Food Chem 2004;52:55−64.
[8] Cleemput MV, Heyerick A, Libert C, Swerts K, Philippe J, Keukeleire DD, et al. D. Hop bitter acids efficiently block inflammation independent of GRalpha, PPARalpha, or PPARgamma. Mol Nutr Food Res 2009;53:1143−55.
[9] Siegel L, Miternique-Grosse A, Griffon C, Klein-Soyer, Stephan D. Antiangiogenic properties of lupulone, a bitter acid of hop cones. Anticancer Res 2008;28:289−94.
[10] Xu SY, Xia TS, Zhang JW, Jiang YP, Wang NN, Xin HL. Protective effects of bitter acids from *Humulus lupulus* L. against senile osteoporosis via activating Nrf2/HO-1/NQO1 pathway in D-galactose induced aging mice. J Funct Foods 2022;94:105099.
[11] Wu KC, Black DM. A perspective on postmenopausal bone loss with aging. J Bone Miner Res 2022;37:171−2.
[12] Saxton RA, Sabatini DM. mTOR signaling in growth, metabolism, and disease. Cell 2017;168:960−76.
[13] Dikic I, Elazar Z. Mechanism and medical implications of mammalian autophagy. Nat Rev Mol Cell Biol 2018;19(6): 349−64.
[14] Li X, Xu JK, Dai BY, Wang XL, Guo QY, Qin L. Targeting autophagy in osteoporosis: from pathophysiology to potential therapy. Ageing Res Rev 2020;62:101098.
[15] Sun XL, Zhang JB, Guo YX, Xia TS, Xu LC, Rahmand K, et al. Xanthohumol ameliorates memory impairment and reduces the deposition of β-amyloid in APP/PS1 mice via regulating the mTOR/LC3II and Bax/Bcl-2 signalling pathways. J Pharm Pharmacol 2021;73:1230−9.
[16] Li WW, Zhang SK, Liu J, Liu YY, Liang QW. Vitamin K2 stimulates MC3T3-E1 osteoblast differentiation and mineralization through autophagy induction. Mol Med Rep 2019; 19:3676−84.
[17] Huang LT, Su W, Wu ZQ, Zheng LD, Lv C. Glucosamine suppresses oxidative stress and induces protective autophagy in osteoblasts by blocking the ROS/Akt/mTOR signaling pathway. Cell Biol Int 2022;46:829−39.
[18] Qi M, Zhang LQ, Ma Y, Shuai Y, Li LY, Luo KF, et al. Autophagy maintains the function of bone marrow mesenchymal stem cells to prevent estrogen deficiency-induced osteoporosis. Theranostics 2017;7:4498−516.
[19] Thomas N, Choi HK, Wei X, Wang L, Mishina Y, Guan JL, et al. Autophagy regulates craniofacial bone acquisition. Calcif Tissue Int 2019;105:518−30.
[20] Xia TS, Lin LY, Jiang YP, Zhang QY, Qin LP, Xin HL. Intervening effects of lupulone and humulone in *Humulus lupulus* L. on osteoblasts and osteoclasts of rats. Acad J Second Mil Med Univ 2019;40:25−30.
[21] Sun XL, Xia TS, Zhang SY, Zhang JB, Xu LC, Han T, et al. Hops extract and xanthohumol ameliorate bone loss induced by iron overload via activating Akt/GSK3β/Nrf2 pathway. J Bone Miner Metab 2022;40:375−88.
[22] Hung YT, Tikhonova MA, Ding SJ, Kao PF, Lan HH, Liao JM, et al. Effects of chronic treatment with diosgenin on bone loss in a D-galactose-induced aging rat model. Chin J Physiol 2014;57:121−7.
[23] Xia TS, Zhang JB, Guo YX, Jiang YP, Qiao FL, Li K, et al. Humulus lupulus L. Extract protects against senior osteoporosis through inhibiting amyloid β deposition and oxidative stress in APP/PS1 mutated transgenic mice and osteoblasts. Molecules 2023;28:583.
[24] Wei WZ, Liu SC, Song J, Feng TQ, Yang R, Cheng YY, et al. MGF-19E peptide promoted proliferation, differentiation and mineralization of MC3T3-E1 cell and promoted bone defect healing. Gene 2020;749:144703.
[25] Maupin KA, Himes ER, Plett AP, Chua HL, Singh P, Ghosh J, et al. Aging negatively impacts the ability of megakaryocytes to stimulate osteoblast proliferation and bone mass. Bone 2019;127:452−9.
[26] Yue C, Jin HT, Zhang X, Li WY, Wang DL, Tong PJ, et al. Aucubin prevents steroid-induced osteoblast apoptosis by enhancing autophagy via AMPK activation. J Cell Mol Med 2021;25:10175−84.
[27] Vardiyan R, Ezati D, Anvari M, Ghasemi N, Talebi A. Effect of L-carnitine on the expression of the apoptotic genes Bcl-2 and Bax. Clin Exp Reprod Med 2020;47: 155−60.
[28] Wang S, Deng ZT, Ma YC, Jin JW, Qi FJ, Li SX, et al. The role of autophagy and mitophagy in bone metabolic disorders. Int J Biol Sci 2020;16:2675−91.
[29] Shi Y, Liu XY, Jiang YP, Zhang JB, Zhang QY, Wang NN, et al. Monotropein attenuates oxidative stress via Akt/mTOR-mediated autophagy in osteoblast cells. Biomed Pharmacother 2020;121:109566.
[30] Yu Q, Shi H, Ding Z, Wang Z, Yao H, Lin R. The E3 ubiquitin ligase TRIM31 attenuates NLRP3 inflammasome activation in Helicobacter pylori-associated gastritis by regulating ROS and autophagy. Cell Commun Signal 2023;21:1.
[31] Schaaf MB, Keulers TG, Vooijs MA, Rouschop KM. LC3/GABARAP family proteins: autophagy-(un)related functions. FASEB J 2016;30:3961−78.
[32] Debnath J, Gammoh N, Ryan KM. Autophagy and autophagy-related pathways in cancer. Nat Rev Mol Cell Biol 2023;24:560−75.
[33] Prerna K, Dubey VK. Beclin1-mediated interplay between autophagy and apoptosis: new understanding. Int J Biol Macromol 2022;204:258−73.
[34] Ma YP, Li CF, He Y, Fu TW, Song L, Ye QS, et al. Beclin-1/LC3-II dependent macroautophagy was uninfluenced in ischemia-challenged vascular endothelial cells. Genes Dis 2021;9:549−61.
[35] Fang SH, Wan X, Zou XY, Sun S, Hao XR, Liang CC, et al. Arsenic trioxide induces macrophage autophagy and atheroprotection by regulating ROS-dependent TFEB nuclear translocation and AKT/mTOR pathway. Cell Death Dis 2021; 12:88.
[36] Ma L, Zhang RX, Li DM, Qiao TT, Guo XY. Fluoride regulates chondrocyte proliferation and autophagy via PI3K/AKT/mTOR signaling pathway. Chem Biol Interact 2021;349: 109659.
[37] Gong W, Liu MQ, Zhang Q, Zhang QL, Wang Y, Zhao QM, et al. Orcinol glucoside improves senile osteoporosis through

attenuating oxidative stress and autophagy of osteoclast via activating Nrf2/Keap1 and mTOR signaling pathway. Oxid Med Cell Longev 2022;2022:5410377.

[38] Yuan YF, Sun JG, Zhou H, Wang S, He CJ, Chen TP, et al. The effect of QiangGuYin on osteoporosis through the AKT/mTOR/autophagy signaling pathway mediated by CKIP-1. Aging (Albany NY) 2022;14:892–906.

[39] Kim JM, Yang YS, Hong J, Chaugule S, Chun H, van der Meulen MCH, et al. Biphasic regulation of osteoblast development via the ERK MAPK-mTOR pathway. Elife 2022;11:e78069.

[40] Huang B, Wang YK, Wang WH, Chen J, Lai PL, Liu ZY, et al. mTORC1 prevents preosteoblast differentiation through the Notch signaling pathway. PLoS Genet 2015;11:e1005426.